Dissipation-scale fluctuations in the inner region of turbulent channel flow

2011 J. Phys.: Conf. Ser. 318 042019

(http://iopscience.iop.org/1742-6596/318/4/042019)

Journal of Physics: Conference Series **318** (2011) 042019 doi:10.1088/1742-6596/318/4/042019

Dissipation-scale fluctuations in the inner region of turbulent channel flow

P. E. Hamlington[1], D. Krasnov[2], T. Boeck[2] and J. Schumacher[2]

[1]Laboratory for Computational Physics and Fluid Dynamics, Naval Research Laboratory, Washington D.C. 20375, USA

[2]Institute of Thermodynamics and Fluid Mechanics, Ilmenau University of Technology, P.O. Box 100565, D-98684 Ilmenau, Germany

E-mail: peterh@lcp.nrl.navy.mil, dmitry.krasnov@tu-ilmenau.de, thomas.boeck@tu-ilmenau.de, joerg.schumacher@tu-ilmenau.de

Abstract. The statistics of intense energy dissipation events in wall-bounded shear flows are studied using highly resolved direct numerical simulations of turbulent channel flow at three different friction Reynolds numbers. Distributions of the energy dissipation rate and local dissipation scales are computed at various distances from the channel walls, with an emphasis on the behavior of the statistics in the near-wall region. The dependence of characteristic mean and local dissipation scales on wall distance is also examined over the full channel height. Systematic variations in these statistics are found close to the walls due to the anisotropy generated by mean shear and coherent vortical structures. Results near the channel centerline are consistent with those found in homogeneous isotropic turbulence.

1. Introduction

Prior numerical and experimental studies (Sreenivasan & Antonia, 1997; Ishihara *et al.*, 2009; Wallace, 2009; Wallace & Vukoslavčević, 2010) have shown that the kinetic energy dissipation rate, $\varepsilon(\mathbf{x},t) \equiv \nu(\partial_i u_j' + \partial_j u_i')^2/2$, in fully developed turbulence is highly intermittent at small scales, where u_i' is the fluctuating velocity and ν is the kinematic viscosity. Consequently, local values of ε that are orders of magnitude larger than the mean value, $\langle\varepsilon\rangle$, occur with substantially higher probability than would be expected if small-scale turbulence were described by Gaussian statistics. These fluctuating amplitudes can be connected to a range of scales, η, over which dissipation occurs. This range of scales is in contrast to the Kolmogorov picture of the turbulent energy cascade (Kolmogorov, 1941), where all dissipation is assumed to take place near the single scale $\eta_K = (\nu^3/\langle\epsilon\rangle)^{1/4}$.

A natural issue arising from this conceptual framework concerns the variation of distributions of η in different flows. Definitions for η have been proposed in the past from consideration of multifractals in turbulence (Paladin & Vulpiani, 1987) and through analogy with η_K (Sreenivasan, 2004). Here we consider distributions of the more recent definition of η from Yakhot (2006), which requires that the local Reynolds number, $Re_\eta = (\delta_\eta u_i)\,\eta/\nu$, associated with flow regions of size η be $O(1)$, where $\delta_\eta u_i = |u_i(x_i+\eta) - u_i(x_i)|$ is a longitudinal velocity increment over η. Physically, η then corresponds to the scale at which viscous dissipation is of the same order as inertial effects (Yakhot & Sreenivasan, 2005). The resulting probability density

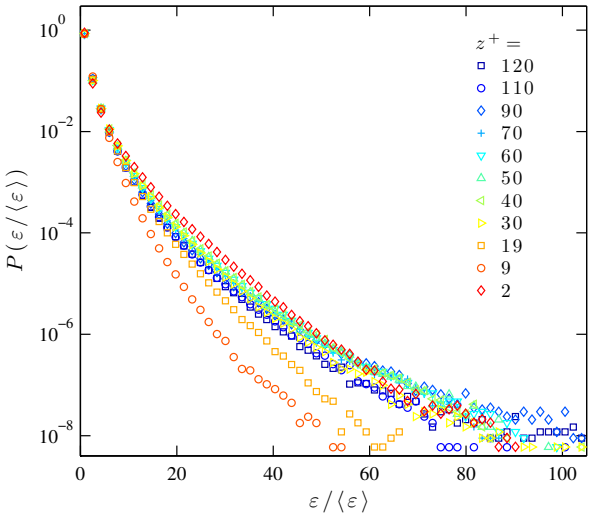

Figure 1. Probability density functions of dissipation rate $\varepsilon/\langle\varepsilon\rangle$ as a function of z^+ in the near-wall region for $Re_\tau = 590$.

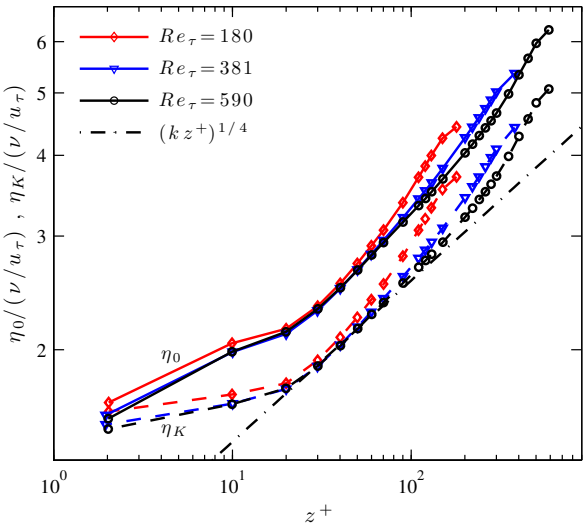

Figure 2. Kolmogorov scale η_K (dashed lines) and the reference scale η_0 (solid lines) as functions of z^+.

functions (pdfs), given by $Q(\eta) = P\,[\eta|(\delta_\eta u_i)\eta/\nu = 1]$, have been calculated previously in several different flows, including homogeneous isotropic turbulence (Schumacher, 2007), turbulent pipe flow (Bailey *et al.*, 2009), and buoyancy-driven turbulence (Zhou & Xia, 2010).

Here we use highly resolved direct numerical simulations (DNS) to examine $Q(\eta)$ and other statistics associated with η in turbulent channel flow at friction Reynolds numbers $Re_\tau = u_\tau L/\nu = 180$, 381, and 590, where u_τ is the friction velocity and L is the channel half-height. We focus here, in particular, on statistics in the near-wall region for $z^+ \lesssim 120$, where $z^+ = u_\tau z/\nu$ and z is the direction normal to the channel walls. This includes the log-layer for $z^+ \geq 30$ and $z/L \lesssim 0.3$, the buffer layer for $30 > z^+ \geq 5$, and the viscous sublayer for $z^+ < 5$ (Pope, 2000). The numerical data used here have also been examined in two previous studies of dissipation and enstrophy statistics (Boeck *et al.*, 2010; Hamlington *et al.*, 2011), and we now include the additional simulation for $Re_\tau = 590$ in the analysis.

2. Channel flow simulations

The numerical simulations used in the present study solve the incompressible Navier Stokes equations for a fully developed turbulent channel flow using a pseudo-spectral method. The method is temporally second-order accurate and uses Fourier expansions in the x and y directions, parallel to the channel walls, and Chebyshev polynomial expansions in the z direction. The grid dimensions are $N_x \times N_y \times N_z = 512 \times 512 \times 1025$ for $Re_\tau = 180$, $1024 \times 512 \times 1025$ for $Re_\tau = 381$, and $2048 \times 1024 \times 2049$ for $Re_\tau = 590$. The number of Fourier or Chebyshev modes in the simulations is 2/3 the grid dimensions as a result of de-aliasing. The size of the simulation domain is $(L_x \times L_y \times L_z)/L = 4\pi \times 2\pi \times 2$ for $Re_\tau = 180$ and $2\pi \times \pi \times 2$ for $Re_\tau = 381$ and $Re_\tau = 590$. The resulting grid spacings are substantially finer than in prior channel flow simulations at comparable values of Re_τ (Moser *et al.*, 1999). Further explanation of the simulations and numerical method is given in Boeck *et al.* (2010) and Hamlington *et al.* (2011).

Temporal snapshots of the flow field are stored every 0.1 convective time units, L/U, for the $Re_\tau = 180$ simulation and approximately every 0.2 units for the other values of Re_τ, where U is the total mean velocity. There are 403 total snapshots for $Re_\tau = 180$, 134 snapshots

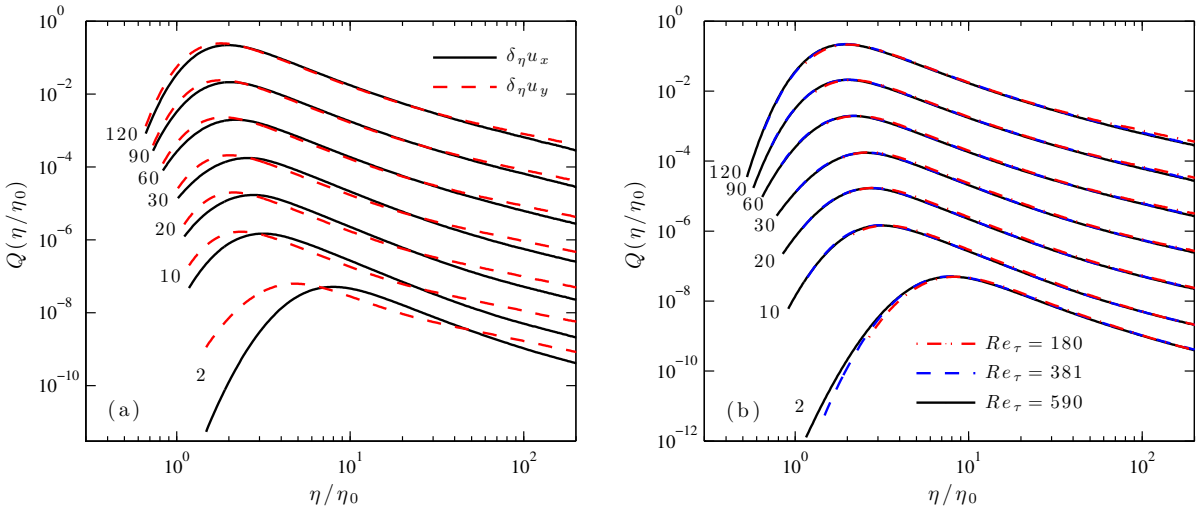

Figure 3. Local dissipation scale pdfs, $Q(\eta/\eta_0)$, as functions of wall distance, z^+ (indicated by labels next to curves). (a) $Q(\eta/\eta_0)$ computed using streamwise (u_x) and spanwise (u_y) velocity increments for $Re_\tau = 381$. (b) $Q(\eta/\eta_0)$ computed using streamwise (u_x) velocity increments for all available Re_τ. Distributions corresponding to different z^+ are shifted down for clarity; pdfs at $z^+ = 120$ are unshifted. The smooth curves in both (a) and (b) are obtained using spline interpolation.

for $Re_\tau = 381$, and 81 snapshots for $Re_\tau = 590$. The statistical analysis is carried out over all available snapshots, and the resulting data for a single horizontal plane (and its symmetry counterpart in the upper half of the channel) then consists of between 1.4×10^8 and 3.4×10^8 total points. The fluctuating velocity is calculated separately in each plane as $u_i' = u_i - \langle u_i \rangle$, where $\langle \cdot \rangle$ is a z-dependent average over time, x-y planes, and symmetric halves of the channel.

3. Results

Figure 1 shows pdfs of $\varepsilon/\langle\varepsilon\rangle$ in the near-wall region ($2 \le z^+ \le 120$) for $Re_\tau = 590$. For intermediate values of $\varepsilon/\langle\varepsilon\rangle$, the pdfs increase from $z^+ = 9$ to 40, before decreasing again slightly up to $z^+ = 120$. The pdf in the viscous sublayer immediately at the wall ($z^+ = 2$), however, is higher in this region than the pdfs for all other values of z^+. The widest tails for large $\varepsilon/\langle\varepsilon\rangle$ are found within the log-layer for $z^+ \approx 90$, consistent with prior results for $Re_\tau = 381$ (Hamlington *et al.*, 2011).

The variation of the Kolmogorov mean dissipation scale, η_K, is shown for the full channel height in Fig. 2. We also show the variation of the reference scale, η_0, used in prior studies of $Q(\eta)$ (Schumacher, 2007; Bailey *et al.*, 2009). Whereas η_K is given by $\eta_K = \ell Re_\ell^{-3/4}$, where $Re_\ell = U_\ell \ell/\nu$, ℓ is the integral length scale, and U_ℓ is the integral velocity scale, η_0 accounts for intermittency corrections (Schumacher, 2007) and scales as $\eta_0 = \ell Re_\ell^{-0.72}$. Here we make the approximation $U_\ell \approx U_{rms}$, where U_{rms} is the z-dependent rms turbulent velocity, which allows η_K and η_0 to be related as $\eta_0/L = (\eta_K/L)^{1.12} Re_{rms}^{0.12}$, where $Re_{rms} = U_{rms} L/\nu$.

Figure 2 shows that both η_K and η_0 increase with distance from the wall. The curves for different Re_τ show generally close agreement in the log-layer, and become substantially different only for larger values of z^+. In the log-layer, η_K is in good agreement with $\eta_K = (kz^+)^{1/4}$, where $k = 0.43$ is the von Karman constant. This relation is a consequence of the $1/z^+$ scaling of $\langle\varepsilon\rangle$ within the log-layer (Pope, 2000). For all locations in the channel and all Re_τ, η_K is about

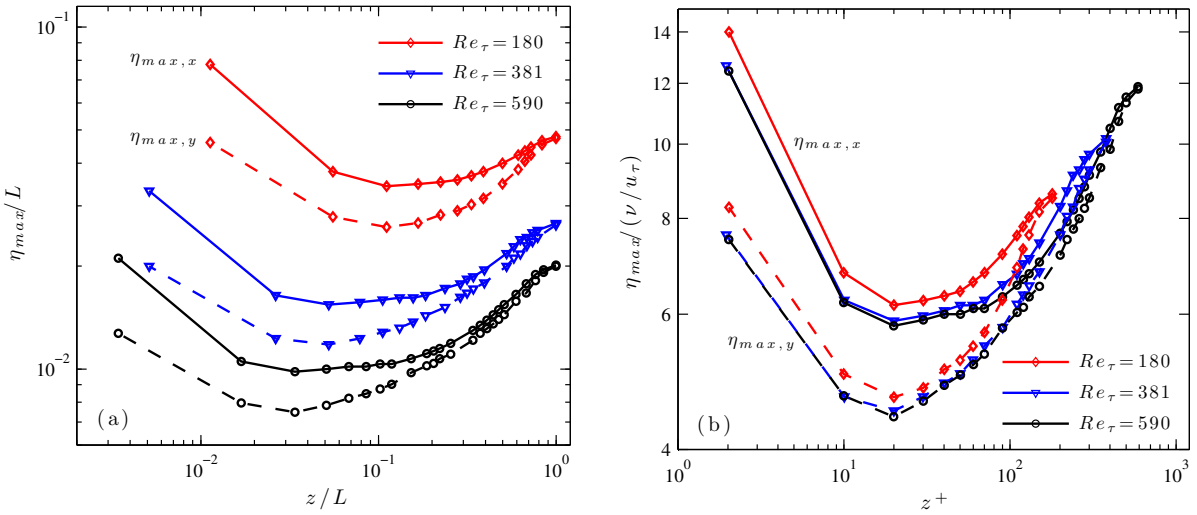

Figure 4. Peak locations $\eta_{max,x}$ and $\eta_{max,y}$ corresponding to maxima in $Q(\eta)$ for streamwise and spanwise velocity increments, respectively, as functions of z in outer units (a) and in friction units (b).

$20-30\%$ smaller than η_0, consistent with results reported for turbulent pipe flow by Bailey *et al.* (2009).

Local dissipation scale pdfs, $Q(\eta)$, are obtained as conditional histograms of η when $(\delta_\eta u_i)\,\eta/\nu$ is in the interval $0.9 \le (\delta_\eta u_i)\,\eta/\nu \le 1.1$. Figure 3(a) shows $Q(\eta/\eta_0)$ calculated using both streamwise, $\delta_\eta u_x = |u_x(x+\eta,y,z,t) - u_x(x,y,z,t)|$, and spanwise, $\delta_\eta u_y = |u_y(x,y+\eta,z,t) - u_y(x,y,z,t)|$, velocity increments for $Re_\tau = 381$. For $z^+ \ge 90$, the peaks of the distributions are located at $\eta \approx 2\eta_0$, and there are only small differences between the streamwise and spanwise pdfs. As the wall is approached, however, the peaks in the pdfs shift to larger values of η/η_0, and there is an accompanying increase in the separation between the streamwise and spanwise pdfs. In particular, the streamwise pdfs are peaked at larger values of η than the spanwise pdfs. These differences may be due to streamwise vortices near the wall, which give smaller differences in u_x, and, hence, larger values of η at which the condition $(\delta_\eta u_i)\,\eta/\nu \approx 1$ is satisfied.

The influence of Reynolds number on $Q(\eta/\eta_0)$ is shown in Fig. 3(b). For the range of wall distances considered, the pdfs essentially collapse, and small variations in the shapes of the curves are only seen within the viscous sublayer at $z^+ = 2$. This suggests that, in the inner region of the channel and outside the viscous sublayer, the shape of $Q(\eta/\eta_0)$ depends only on wall distance when z is normalized in friction units.

The peak locations of the pdfs in Fig. 3, denoted $\eta_{max,x}$ and $\eta_{max,y}$ for the streamwise and spanwise pdfs, respectively, are shown in Fig. 4 for all Re_τ. Figure 4(a) shows that, as the wall is approached from the centerline, both $\eta_{max,x}$ and $\eta_{max,y}$ decrease, before increasing again very near the wall. At the same time, however, the differences between $\eta_{max,x}$ and $\eta_{max,y}$ become increasingly large as the wall is approached. This is indicative of the increasing influence of anisotropy generated by mean shear. Nearly identical values of $\eta_{max,x}$ and $\eta_{max,y}$ are only seen very close to the channel centerline where the mean shear and anisotropy are small.

Figure 4(a) shows that normalization of $\eta_{max,x}$ and $\eta_{max,y}$ using outer units does not reveal a distinct location, z/L, where the differences between $\eta_{max,x}$ and $\eta_{max,y}$ cease to be significant. Normalization by friction units in Fig. 4(b), however, gives a somewhat clearer indication that substantial differences between $\eta_{max,x}$ and $\eta_{max,y}$ begin to occur, for all Re_τ, at $z^+ \approx 100$. This normalization also shows that the variations of $\eta_{max,x}$ and $\eta_{max,y}$ are similar for the higher values

of Re_τ, and that there is an approximate plateau in $\eta_{max,x}$ over the interval $20 \lesssim z^+ \lesssim 70$.

4. Conclusions

Local dissipation scale pdfs in the near-wall region of turbulent channel flow show systematic variations with wall distance. When the wall distance is normalized by friction units, the shape of the pdfs at each z^+ appears to be only weakly dependent on Re_τ. Within the near-wall region, pdfs constructed using streamwise and spanwise velocity increments show differences that reflect the presence of coherent structures in the logarithmic and buffer layers. These differences decrease, however, near the centerline as the anisotropy generated by the mean shear decreases. Additional study is required to fully characterize the details of this continuous transition from anisotropic, shear-dominated turbulence in the near-wall region to homogeneous and isotropic statistics at the centerline. A more detailed investigation including additional results will be reported elsewhere (Hamlington *et al.*, in preparation).

Acknowledgments

We thank the DEISA Consortium (www.deisa.eu), co-funded through the EU FP6 project RI-031513 and the FP7 project RI-222919, for support within the DEISA Extreme Computing Initiative. The computations were carried out on the Cray XT4 Cluster Hector at EPCC in Edinburgh. We wish to thank Florian Janetzko for assistance with the parallel input/output routines. PEH was supported by a National Research Council Research Associateship Award at the Naval Research Laboratory. DK and TB were supported by the Deutsche Forschungsgemeinschaft (DFG). JS acknowledges support by the Heisenberg-Program of DFG.

References

Adrian, R. J. 2007 *Phys. Fluids* **19**, 041301.

Bailey, S. C. C., Hultmark, M., Schumacher, J., Yakhot, V. and Smits, A. J. 2009 *Phys. Rev. Lett.* **103**, 014502.

Boeck, T., Krasnov, D. and Schumacher, J. 2010 *Physica (Amsterdam)* **239D**, 1258.

Hamlington, P. E., Krasnov, D., Boeck, T. and Schumacher, J. 2011 *Physica D (Amsterdam)*, DOI 10.1016/j.physd.2011.06.012.

Hamlington, P. E., Krasnov, D., Boeck, T. and Schumacher, J. Local dissipation scales and energy dissipation statistics in turbulent channel flow (in preparation).

Ishihara, T., Gotoh, T. and Kaneda, Y. 2009 *Annu. Rev. Fluid Mech.* **41**, 165.

Kolmogorov, A. N. 1941 *Dokl. Akad. Nauk SSSR* **30**, 299.

Moser, R. D., Kim, J. and Mansour, N. N. 1999 *Phys. Fluids* **11** (4), 943.

Paladin, G. and Vulpiani, A. 1987 *Phys. Rev. A* **35**, 1971.

Pope, S. B. 2000, *Turbulent flows.* Cambridge University Press.

Schumacher, J. 2007 *Europhys. Lett.* **80**, 54001.

Sreenivasan, K. R. 2004 *Flow Turb. Combust.* **72**, 115.

Sreenivasan, K. R. and Antonia, A. R. 1997 *Annu. Rev. Fluid Mech.* **29**, 435.

Wallace, J. M. 2009 *Phys. Fluids* **21**, 021301.

Wallace, J. M. and Vukoslavčević, P. V. 2010 *Annu. Rev. Fluid Mech.* **42**, 157.

Yakhot V. and Sreenivasan, K. R. 2005 *J. Stat. Phys.* **121** (5), 823.

Yakhot, V. 2006 *Physica (Amsterdam)* **215D**, 166.

Zhou, Q. and Xia, K.-Q. 2010 *Phys. Rev. Lett.* **104**, 124301.